

**NASA TECHNICAL
MEMORANDUM**

N72-31885
NASA TM X-62,181

NASA TM X-62,181

**CASE FILE
COPY**

**SEPARATION AND COMMUNICATIONS GEOMETRY ANALYSIS FOR
A JUPITER ENTRY PROBE FROM A PIONEER SPACECRAFT**

Edward L. Tindle

Ames Research Center
Moffett Field, Calif. 94035

September 1972

INTRODUCTION

Recently, as part of the development of an overall exploration strategy for the outer planets, considerable scientific interest has been exhibited in performing in-situ measurements with probes within the atmospheres of Jupiter and the other giant planets. Initially, attention was focussed upon the preliminary feasibility of such missions (e.g., refs. 1-3). Having demonstrated that feasibility, attention has been recently directed toward obtaining maximum scientific benefit from such missions for the lowest cost. In that regard, the feasibility and the capability of performing an atmosphere-entry probe mission to Jupiter utilizing a modified version of the existing Pioneer Jupiter spacecraft has been performed. The Pioneer spacecraft is a spinning spacecraft with its axis of spin continually directed at Earth and therefore the appropriate separation of the probe for entry and the appropriate phasing of probe and spacecraft for relay communications is a unique and previously unanalyzed problem. The purpose of this paper is to present a complete analysis of this problem.

DISCUSSION

There are two basic approaches toward separating the probe for entry: (1) the deflected probe mode where the bus and probe are targeted along an appropriate nonimpacting trajectory and, at some distance prior to encounter, the probe is separated and deflected onto an impacting trajectory, and (2) the deflected bus mode where the bus and probe are targeted for entry and, at some distance prior to entry, the probe is separated and the bus is deflected to an appropriate nonimpacting trajectory. Both these approaches are discussed in detail in reference 1 for a three-axis stabilized vehicle. For an Earth-line spinning vehicle, however, the separation and phasing problem is considerably different. These two approaches will be discussed for a nominal, close flyby trajectory and for a high flyby trajectory to avoid a possible radiation hazard.

Deflected Probe Mode. - For the deflected probe mode with a spinning spacecraft, the deflection maneuver is constrained by the fact that the deflection velocity increment must be added to the probe in the direction of the spin axis. (This assumes that the probe is not capable of attitude control changes which is consistent with the concept of a simple inexpensive probe). In general, this results in both a deflection of the probe toward the planet and an acceleration of the probe along its flight path. This increases the lead time of the probe and would place it at entry before the bus is in position to receive communications. Therefore the bus must also be accelerated along its flight path after the deflection has occurred in order to compensate for this lead time.

The geometry of the deflection and phasing maneuvers for the deflected probe mode is shown in figure 1. Line-of-sight communications are to be maintained continuously (except for blackout) between separation and the time the design pressure is reached by the appropriate choice of the phasing maneuver, ΔV_p . The mathematical development of the analysis of the appropriate deflection maneuver for the probe and the phasing maneuver for the bus is fully developed in the Appendix. The analysis first determines the probe entry conditions (entry angle and angle of attack) for a given deflection maneuver from a given bus trajectory.

With the goal of achieving reasonable science goals at minimum cost in terms of weight and technological complexity, a design pressure of 10 bars was chosen as a reasonable survival goal. Design for higher survival pressures involves the use of a pressure shell to protect the instrumentation with attendant greater weight requirements. In addition, the increase of atmospheric attenuation of RF signals below the 10 bar level markedly decreases the communications margin. The nominal descent time requirements from entry to the 10 bar level is about 20 minutes.

In order to determine the probe deflection requirements, the spacecraft phasing strategy, and the resulting communication geometry, nominal arrival conditions corresponding to a trip time of 800 days for a launch during the 1978 opportunity were assumed. This trip time corresponds to a nearly minimum energy Type I transfer for that launch opportunity. This is also one of the missions analyzed in reference 1 and thus allows comparison with similar requirements for a three-axis stabilized vehicle. In reference 1 it is shown that separating the probe at a distance from Jupiter of $100 R_J$ (Jupiter radii) results in reasonable deflection velocity requirements without undue errors in entry angle. In addition, it is also shown that a flyby periapsis radius of about $1.3 R_J$ is the closest passage which can be made (thereby reducing communications range) which will allow a line-of-sight communications link to the probe within reasonable antenna constraints. This separation distance and flyby periapsis radius were thus assumed as nominal conditions in the calculations that follow.

In order to simplify the calculations by making the problem planar, the bus and probe orbit plane was chosen such that it contained the spin axis. For the 1978 opportunity, this resulted in a flyby orbit inclination of 7.7° . This flyby trajectory would also cause the bus to be diametrically occulted from the Earth by Jupiter. Figure 2 shows, for the nominal mission and separation conditions, the relative entry angle and angle of attack achieved by the probe for a variety of deflection ΔV 's with the steeper entries, of course, requiring the higher ΔV 's. Note that zero angle of attack occurs for a relative entry flight path angle of about -25.5° . Aerodynamic stability is enhanced for the entry probe with an angle of attack near zero. Reference 1 shows that entry angles between -15° and -30° are the most desirable considering factors such as entry deceleration, entry thermal protection, communications margin, and guidance and control accuracies. It appears, then, that nearly ideal entry conditions can be obtained for a deflected probe from this nominal mission.

Trip times and bus pericenter radii were varied parametrically from the nominal values. The curve in figure 2 depends only slightly on bus pericenter radius from 1.2 to about $2 R_J$. The variation of entry angle as a function of trip time for fixed values of entry angle of attack near zero is shown in figure 3. It is seen that the 800 day trip is about the shortest to yield reasonable entry angles ($20-25^\circ$) for zero angle of attack. Figure 4 shows that for trip times from 750 to 850 days that the deflection velocity decreases for the longer trips. Figure 5 shows the effect of bus periapsis radius (up to $2 R_J$) on deflection ΔV to achieve entry angles of attack of -10° , 0° and $+5^\circ$ for the 800 day nominal trip to Jupiter. From the results of figures 2-4 it appears that the choice of nominal mission parameters as indicated in reference 1 is also a very reasonable choice for the case of deflection from a spinning spacecraft.

After examining the probe deflection, the appropriate phasing of the bus and the resulting communications geometry (also described in the appendix) is analyzed. In order to simplify the probe's antenna design, the bus was phased to limit the probe look angle to about $\pm 45^\circ$ during the probe's descent. At the same time, the phasing maneuver was sized to minimize the probe-to-bus communications range at 20 minutes after entry. This minimizes the effect of space loss attenuation when the probe is at the design depth of 10 bars with its signal facing maximum atmospheric attenuation. This phasing ΔV of about 100 m/sec was applied to the spacecraft in the flyby plane at about 114° relative to the spin axis such that the spacecraft was speeded up.

The resulting communications geometry is characterized by two aspect or look angles. The bus aspect angle is the angle between the bus spin axis and the bus-to-probe line, while the probe aspect angle is the angle between the probe spin axis and the probe-to-bus line (see figure 6). To maintain its Earth-link, the bus always points with its spin axis toward the Earth. Figure 7 shows the bus and probe aspect angles for times near entry for the appropriately phased

trajectory from the nominal mission. Since both the probe and the bus are stabilized and spinning about Earth-directed lines, the probe and bus look angles are equal before entry and are about 40° for the phasing shown. At entry the probe's spin axis is essentially along the Earth line. After deceleration, the probe's spin axis points away from Jupiter's center and the probe is carried along by the Jovian atmosphere. This rapid change in probe aspect angle is seen in figure 7. The high speed of the bus relative to the decelerated probe causes both aspect angles to increase more rapidly after entry.

Figure 8 shows the range and range rate (rate of change of the communications range) for times near entry. The change in range rate from the time of entry to that associated with the terminal descent is a measure of the doppler shift that must be tracked to reacquire the signal after blackout. Note that at 20 minutes after entry, the probe and bus look angles have increased to about 10° and 90° respectively. The data of figures 7 and 8 are used to design the antenna and communications system of bus and probe and to define the margin for the system.

An estimate of the telemetry link performance margin has been made for the nominal mission. The factors included in the estimation of the acquisition signal-to-noise ratio, from which the margin is obtained, are as follows: (1) probe transmitter power of 40 watts; (2) data rate of 50 bits/second; (3) carrier frequency of 1 GHz; (4) maximum communications range of 60,000 km; (5) total system loss of 2.5 dB; (6) telemetry modulation loss of 3 dB; (7) a fixed, circularly polarized probe antenna with a peak gain of 10 dB at 18° off axis mounted such that the beam is symmetrical with respect to the spin axis; (8) a broadbeam bus antenna (to cover the 60° change in bus aspect angle during the probe's descent) with a peak gain of 4.5 dB mounted off the bus spin axis but such that the beam pattern is symmetric about the axis. The above described telemetry link provided at least 7 dB margin over the threshold signal-to-noise ratio for the nominal mission to 10 bars. This includes attenuation of no more than 1 dB for the worst model atmosphere.

A 7 dB margin is adequate to overcome adverse equipment tolerances, separation and deflection errors and other mission uncertainties. As a result, this communications system for the nominal mission is sufficient to guarantee successful telemetry.

Deflected Bus Mode. - For the deflected bus mode with a spinning spacecraft, the analysis of the appropriate deflection maneuver for the bus is exactly the same as presented in Appendix B of reference 1, if the velocity increment for deflection can be applied in any direction relative to the axis of spin of the spacecraft. This is possible with the Pioneer spacecraft by appropriately pulsing the attitude control jets each revolution for several revolutions in order to obtain the appropriate incremental velocity vector direction and magnitude.

The only difference then with a spinning spacecraft utilizing the deflected bus mode from a three-axis stabilized vehicle using the same mode is that the probe spin axis must be aligned with the Earth line at the time of separation. This constraint eliminates the freedom to target for and achieve a zero angle of attack at entry for any entry angle. This, however, does not present a severe problem as can be seen by referring again to figure 2. Since separation of the probe occurs at a large distance from the planet, the geometric relationship between the entry angle and the entry angle of attack is essentially invariant with the probe separation mode. Therefore figure 2 is a very close representation of that geometric relationship for the deflected bus mode. Entry angles of attack within the range of $\pm 5^\circ$ are achievable for entry path angles over a wide range between -15° and -35° . It is possible to achieve an even wider range of entry angles for low angle of attack by varying trip time at some penalty in launch energy as previously shown in figure 3. But since entry angles between -15° and -30° are the most desirable (ref. 1), it is reasonable to stay within this range and simultaneously achieve small entry angles of attack for the least launch energy.

After separation of the probe, communications between the entry probe and the flyby bus will be maintained by appropriate phasing of the deflected flyby trajectory to keep line-of-sight between these two vehicles during the entire flight to entry and the descent to the design depth with given antenna constraints. The geometry of the deflection and phasing problem for the deflected bus is shown in figure 9 where V_p is the phasing component of the total deflection velocity applied to the bus. The mathematical development of the analysis of the appropriate deflection and phasing maneuver is given in Appendix B of reference 1.

Figure 10 shows the bus deflection ΔV (including the appropriate phasing component) required to deflect the bus trajectory to a variety of periapsis flyby radii for the 1978, 800 day trip to Jupiter. Requirements are shown for entry targetings of -30° and -15° inertial entry flight path angle. Higher separation velocities are required for larger flyby radii and for steeper entry angles. The -30° entry angle curve shown corresponds to a relative entry angle of about -37.5° with an entry angle of attack of -6.5° , while the -15° inertial entry angle corresponds to a -19° relative angle and about $+3^\circ$ angle of attack (see figure 2).

Because of the essential invariance relative to the separation mode, the results of the communications geometry presented in figures 7 and 8 are essentially the same as for a deflected bus mode for the nominal mission. This was verified by doing the geometry analysis by the method described in the Appendix of this report and by that described in Appendix B of reference 1. Table 5 of reference 1 shows that the probe and bus antenna angles for 3-axis stabilized buses are nearly identical for the deflected probe and deflected bus modes of separating the probe for entry. Therefore, the discussion of figures 7 and 8 of the previous section, as well as the resulting communication margin, applies to the deflected bus mode described in this section. Only the deflection and phasing velocity requirements are different.

Special Considerations. - The flyby bus for the nominal mission discussed previously does pass through the postulated Jupiter trapped radiation belts. This section discusses the effects on the mission design of increasing the bus flyby radius in order to avoid the possibly high radiation hazard inherent in the nominal mission. Figure 11 shows the probe and bus aspect angles near the time of entry for a mission which has a bus flyby radius of $6 R_J$, an 800 day trip time for the 1978 opportunity, and which separates the probe at $700 R_J$. The separation radius had to be increased from the $100 R_J$ nominal in order to keep the deflection ΔV required down to a value near that shown in figure 5 for the nominal $1.3 R_J$ flyby mission. For this high flyby radius alternative, the bus aspect angle is about 90° and changes very little from an hour before entry until the mission ends. The range and range rate variation near entry are shown in figure 12 for this mission. Note the large range penalty (nearly 10-fold over that for the $1.3 R_J$ nominal flyby) caused by the high flyby radius. This geometry and large communications range (requiring the bus antenna to have high gain at 90° from the spin axis) requires that the bus antenna be despun either mechanically or electronically in order to achieve a margin comparable to the close flyby mission.

CONCLUSIONS

The separation and communications geometry analysis presented here has shown that it is possible to target a Jupiter entry probe from a Pioneer spin-stabilized vehicle to desired entry conditions and maintain a continuous line-of-sight communications link while the probe descends to a pressure of 10 bars within the atmosphere. Such a targeting is possible with either the deflected probe mode or with the deflected bus mode.

For the nominal mission studied--an 800 day trip in 1978 with the Pioneer type spacecraft flying by at $1.3 R_J$ --it was possible to achieve entries near zero angle of attack at about -25° relative entry flight

path angle. Because of the constraint on the deflection maneuver for the deflected probe mode, the deflection and phasing velocity requirements are much larger for this mode. Otherwise, there is not much to recommend one mode over the other. The geometry parameters--look angles, ranges and range rates--provided by this analysis permit the design of a functional communications system for the bus and probe. Avoiding a high trapped radiation belt hazard at Jupiter by flying the bus by at $6 R_J$, however, requires using a despun antenna on the flyby bus.

REFERENCES

1. Swenson, B. L., et. al.: Preliminary Analysis of an Atmosphere-Entry Probe Mission to Jupiter, NASA TM X-2338, September, 1971.
2. Jupiter Atmospheric Entry Mission Study, Martin Marietta Denver Division, Contract JPL 952811, April, 1971.
3. A Study of a Jupiter Atmospheric Entry Probe Mission, Avco Systems Division, Contract NAS7-100 JPL 952897, August, 1971.

APPENDIX
DEFLECTED PROBE FROM A SPINNING SPACECRAFT

Figure 13 shows schematically the communications geometry for the deflected probe from a spinning spacecraft with its spin axis directed toward Earth. It is assumed that the separation ΔV is applied along the spin axis direction. It is desired to calculate the angle of attack of the probe at entry (the angle between the probe spin axis direction and the relative entry velocity vector) given the separation ΔV and distance, the bus trajectory, the approach asymptote, and the date of arrival. It is also desired to phase the bus trajectory so that a favorable communications link can be obtained during the probe's descent.

The angle of attack at entry, α_e , is obtained using the vector diagrams in figure 13. The plane of the paper in figure 13 is the trajectory plane for the bus and the probe, and in order to reduce the problem to a planar treatment, the plane contains the Earth line. In addition, since the arrival declinations at Jupiter are very small and since the entry trajectory is nearly equatorial, the velocity vector of the rotating atmosphere is assumed to be in the probe trajectory plane. These assumptions greatly simplify the problem and lead to insignificant errors. The requirement that the spacecraft spin axis be in the trajectory plane means that the unit vector normal to the plane, \hat{n} , is defined as follows:

$$\hat{n} = (\hat{r}_E \times \hat{V}_\infty) / \sin \lambda \quad (A1)$$

where

$$\lambda = \cos^{-1} (\hat{r}_E \cdot \hat{V}_\infty)$$

and \hat{r}_E is in the direction of Earth from Jupiter and \hat{V}_∞ is in the direction of the approach asymptote.

To define the vector in the direction of the bus periapsis, \hat{r}_p , we find

$$\epsilon = \cos^{-1} \left(\frac{1}{e_B} \right) \quad (A2)$$

where

$$e_B = 1 - r_p/a_B$$

with

$$a_B = -\mu/V_\infty^2$$

Then \hat{r}_p is normal to \hat{n} and an angle ϵ behind \hat{V}_∞ (A3)

To define \hat{r}_s , in the direction of radius of separation, calculate θ_{SB} , bus true anomaly at separation,

$$\theta_{SB} = \cos^{-1} \left[\left(\frac{a_B \{1 - e_B^2\}}{r_s} - 1 \right) \left(\frac{1}{e_B} \right) \right]$$

Then \hat{r}_s is normal to \hat{n} and an angle θ_{SB} ahead of \hat{r}_p . (A4)

To find \hat{V}_1 , in the direction of the bus velocity at separation, solve for γ_{SB} , bus flight path angle at separation,

$$\gamma_{SB} = \tan^{-1} \left[\frac{e_B \sin \theta_{SB}}{1 + e_B \cos \theta_{SB}} \right]$$

Then \hat{V}_1 is normal to \hat{n} and an angle $90 - \gamma_{SB}$ ahead of \hat{r}_s (A5)

The angle β is defined by

$$\beta = \sin^{-1} \left(\frac{\hat{r}_E \times \hat{V}_1}{\hat{n}} \right); \quad \beta = \cos^{-1} (\hat{r}_E \cdot \hat{V}_1) \quad (A6)$$

To find the direction of the probe radius vector at entry, \hat{r}_e , one needs the true anomaly at separation and entry, θ_{SP} , θ_{ep} .

$$V_1^2 = \mu \left(\frac{2}{r_s} - \frac{1}{a_p} \right)$$

$$V_2^2 = V_1^2 + \Delta V^2 - 2 V_1 \Delta V \cos \beta$$

$$a_p = 1 / (2/r_s - V_2^2/\mu)$$

$$\Delta \gamma = \sin^{-1} \left[\frac{\Delta V}{V_2} \sin \beta \right]$$

Then

$$\gamma_{SP} = \gamma_{SB} - \Delta \gamma$$

Then the eccentricity of the probe's trajectory is given by

$$e_p = \left[1 + \frac{1 - \frac{2 a_p}{r_s}}{(a_p/r_s)^2 (\tan^2 \gamma_{SP} + 1)} \right]^{\frac{1}{2}} \quad (A7)$$

and as before for the bus

$$\theta_{SP} = \cos^{-1} \left[\left(\frac{a_p}{r_s} \{1 - e_p^2\} - 1 \right) \left(\frac{1}{e_p} \right) \right]$$

$$\theta_{ep} = \cos^{-1} \left[\left(\frac{a_p}{r_e} \{1 - e_p^2\} - 1 \right) \left(\frac{1}{e_p} \right) \right]$$

$$\gamma_e = \tan^{-1} \left[\frac{e_p \sin \theta_{ep}}{1 + e_p \cos \theta_{ep}} \right]$$

From figure 13 and noting the previously mentioned simplifying assumptions, it can be seen that the entry angle relative to the rotating atmosphere is

$$\gamma_{er} = \tan^{-1} \left[\frac{V_e \sin \gamma_e}{V_e \cos \gamma_e - V_A} \right] \quad (A8)$$

where

$$V_e^2 = \mu \left(\frac{2}{r_e} - \frac{1}{a_p} \right)$$

V_A = rotation speed of the atmosphere

$$V_A = 2\pi R_J / P_J$$

where P_J = rotation period of planet

R_J = planet radius

To find the angle of attack at entry, it is required to find $\hat{V}_{e,r}$, the unit vector in the direction of the relative velocity at entry. From the vector diagram in the upper left of figure 13 it follows that

$$\bar{V}_{e,r} = V_e \hat{V}_e - V_A \hat{V}_A \quad (A9)$$

where

\hat{V}_e , the direction of the inertial entry velocity, is constructed normal to \hat{n} and $(90 - \gamma_e)$ ahead of \hat{r}_e , and

\hat{V}_A , the direction of the atmosphere's velocity, is normal to \hat{n} and normal to \hat{r}_e

where

\hat{r}_e , the direction of the radius vector of the probe at entry, is normal to \hat{n} and $(\theta_{ep} - \theta_{sp})$ ahead of \hat{r}_s

Then from figure 13 it is seen that the entry angle of attack, α_e , is defined by

$$\begin{aligned}\alpha_e &= \cos^{-1} \left[\hat{r}_E \cdot -\hat{v}_{e,r} \right] \\ \alpha_e &= \sin^{-1} \left[\frac{\hat{r}_E \times -\hat{v}_{e,r}}{\hat{n}} \right]\end{aligned}\tag{A10}$$

It is often required to speed up the bus shortly after separation in order to achieve the proper communications link during the post-entry descent phase. It is assumed that any required phasing ΔV , ΔV_p , is applied along the bus flight path--see figure 13. If a phasing ΔV is applied to the bus, the trajectory is changed and the new trajectory is defined as follows:

$$\begin{aligned}V_1' &= V_1 + \Delta V_p \\ a_B' &= 1/(2/r_s - V_1'^2/\mu) \\ e_B' &= \left[\left(\frac{r_s V_1'^2}{\mu} - 1 \right)^2 \cos^2 \gamma_{SB} + \sin^2 \gamma_{SB} \right]^{\frac{1}{2}} \\ \theta_{SB} &= \cos^{-1} \left[\left(\frac{a_B'}{r_s} \{1 - e_B'^2\} - 1 \right) \left(\frac{1}{e_B'} \right) \right] \\ r_p' &= a_B' (1 - e_B')\end{aligned}$$

At the time when the probe enters the atmosphere, the bus must be located on its trajectory. The time from separation is known and the bus true anomaly, θ_{Be} , is found iteratively from the hyperbolic time equation. The radius of the bus when the probe enters, r_{Be} , is computed once θ_{Be} is known.

$$r_{Be} = a_B' (1 - e_B'^2) / (1 + e_B' \cos \theta_{Be})$$

Then \hat{r}_{Be} is normal to \hat{n} and θ_{Be} from \hat{r}_p

Then to calculate the direction of the probe-to-bus vector, \hat{r}_{pB} ,

$$\bar{r}_{pB} = r_{Be} \hat{r}_{Be} - r_e \hat{r}_e$$

$$\hat{r}_{pB} = \bar{r}_{pB} / |\bar{r}_{pB}|$$

where $|\bar{r}_{pB}| = \text{communications range}$

Then to establish the direction of the bus velocity vector, \hat{V}_B , the bus flight path angle, γ_B , is calculated by

$$\gamma_B = \tan^{-1} [e_B' \sin \theta_{Be} / (1 + e_B' \cos \theta_{Be})]$$

Then \hat{V}_B is normal to \hat{n} and $90 - \gamma_B$ from \hat{r}_{Be}

while

$$V_B = \left[\mu \left(\frac{2}{r_{Be}} - \frac{1}{a_B} \right) \right]^{\frac{1}{2}}$$

Then the direction of the velocity of the probe relative to the bus, \hat{V}_{pB} , is found from

$$\bar{V}_{pB} = V_B \hat{V}_B - V_e \hat{V}_e$$

Then

$$\hat{V}_{pB} = \bar{V}_{pB} / |\bar{V}_{pB}|$$

Note that the range rate is given by

$$\hat{r}_{pB} \cdot \bar{V}_{pB}$$

Continuing with the descent communications geometry, look angles are determined.

The bus aspect angle, ϕ , is defined as shown in figure 14 and calculated by

$$\phi = \cos^{-1} (\hat{r}_E \cdot \hat{r}_{PB})$$

$$\phi = \sin^{-1} (\hat{r}_E \times \hat{r}_{PB} / \hat{n})$$

The probe aspect angle, ω , is found once we know ψ .
where

$$\psi = \cos^{-1} (\hat{r}_e \cdot \hat{r}_{PB})$$

$$\psi = \sin^{-1} (\hat{r}_e \times \hat{r}_{PB} / \hat{n})$$

$$\omega = \psi + 90 + \gamma_r + \alpha$$

where

α = angle of attack

γ_r = relative flight path angle

When the probe is at or before entry

$$\omega = \phi = \psi + 90 + \gamma_r + \alpha$$

after the probe has reached equilibrium descent,

$$\omega = \psi$$

Note that when $\psi > 0$ that the bus is leading the probe.

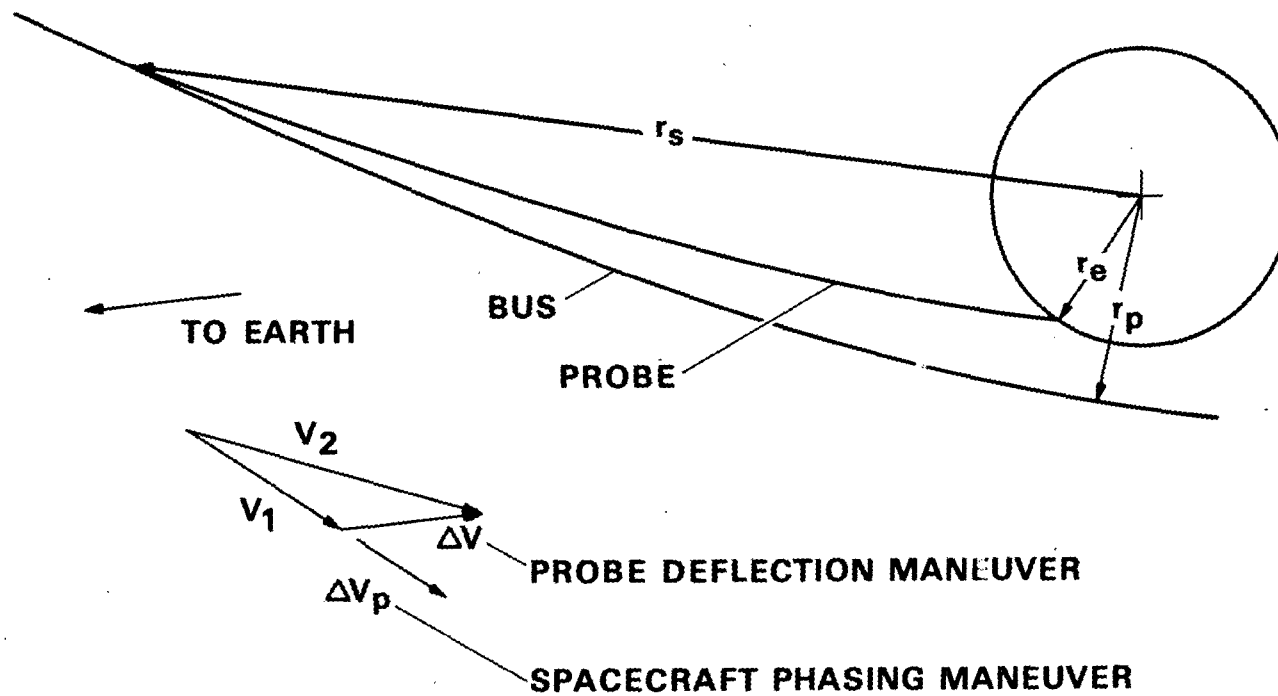


Figure 1. - Deflected Probe.

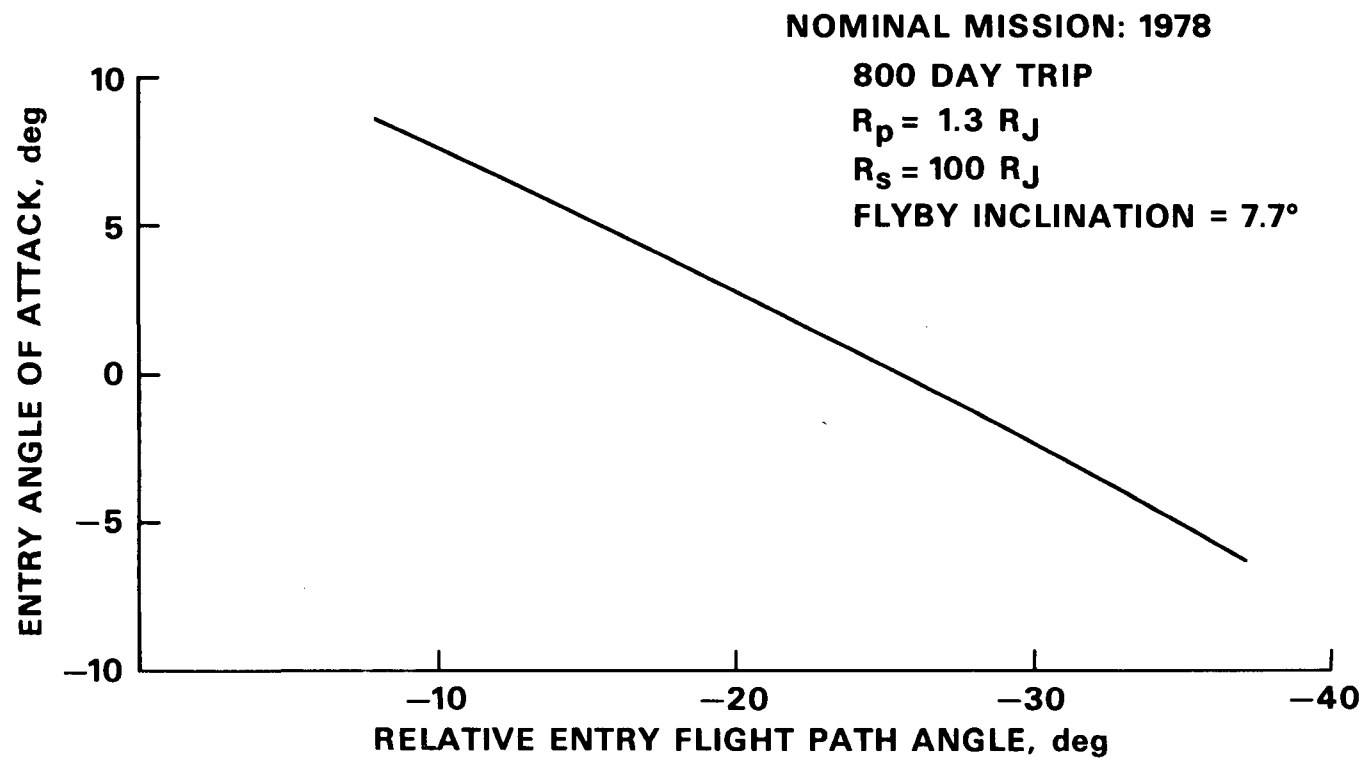


Figure 2. - Angle of Attack at Entry.

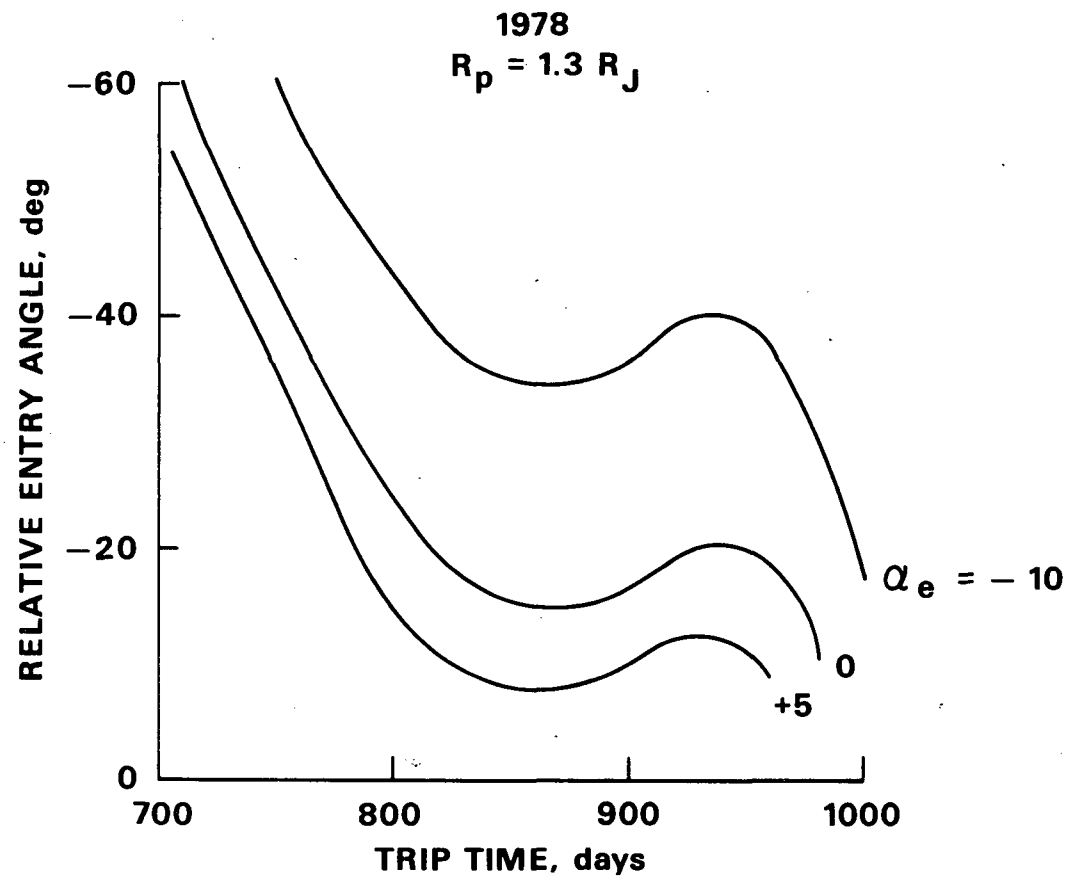


Figure 3. - Trip Time Effect on Nominal Mission.

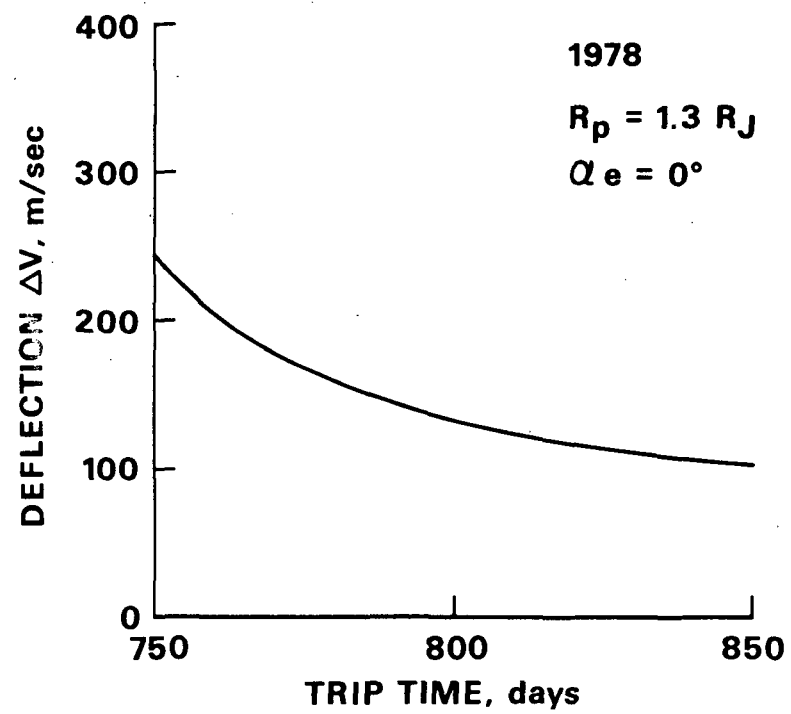


Figure 4. - Deflected Probe ΔV Requirements.

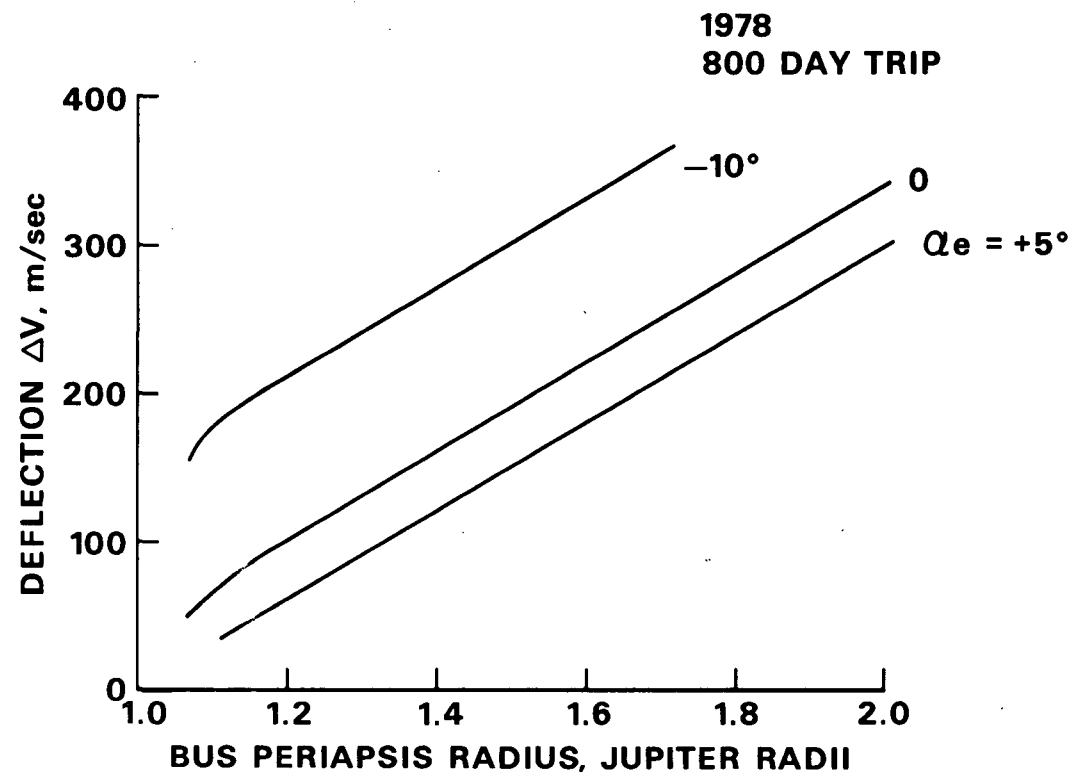


Figure 5. - Probe Deflection ΔV .

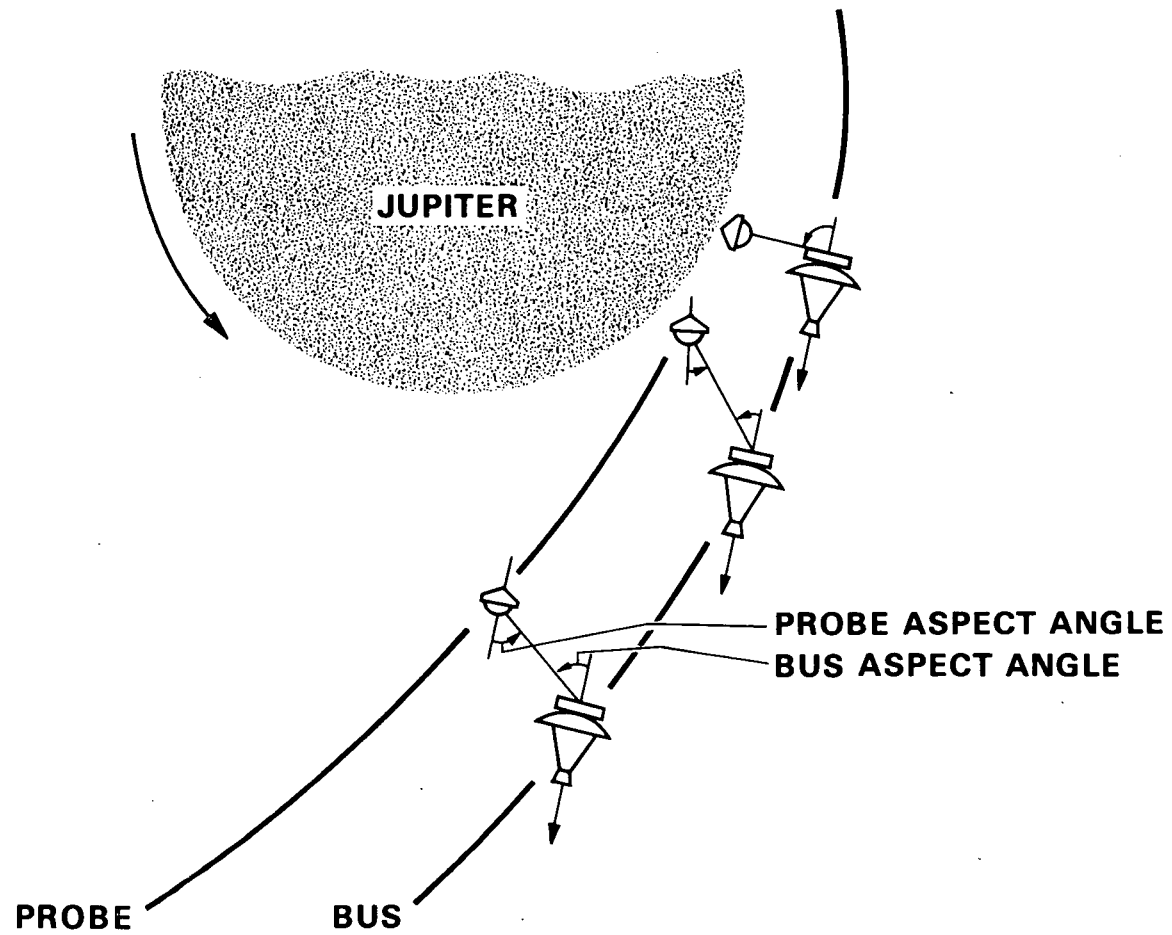


Figure 6. - Antenna Aspect Angles.

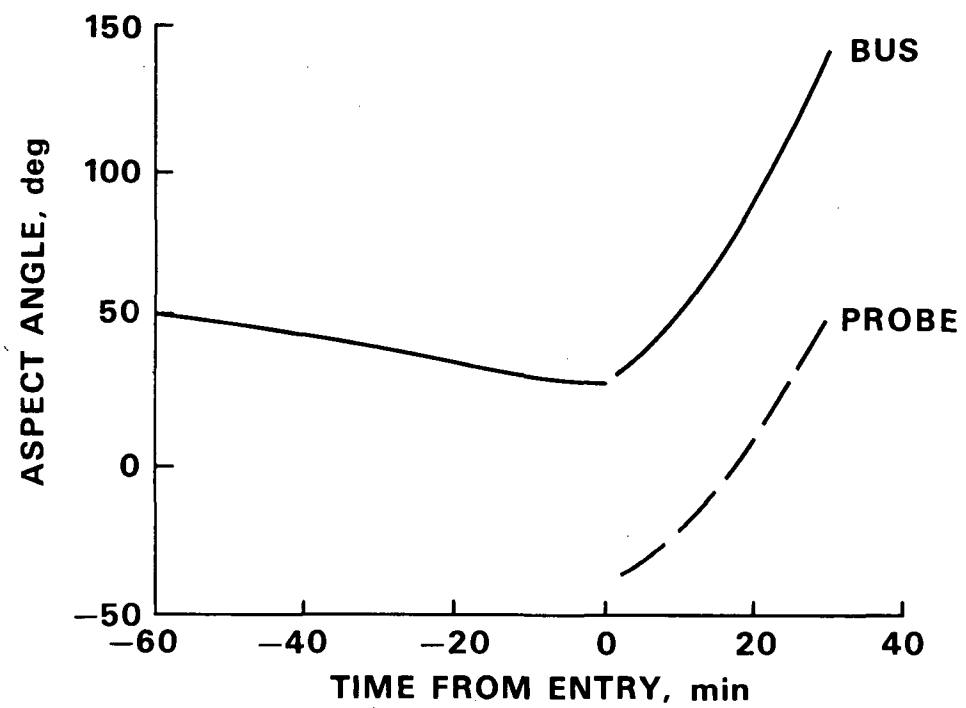


Figure 7. - Communications Geometry; Nominal Mission.

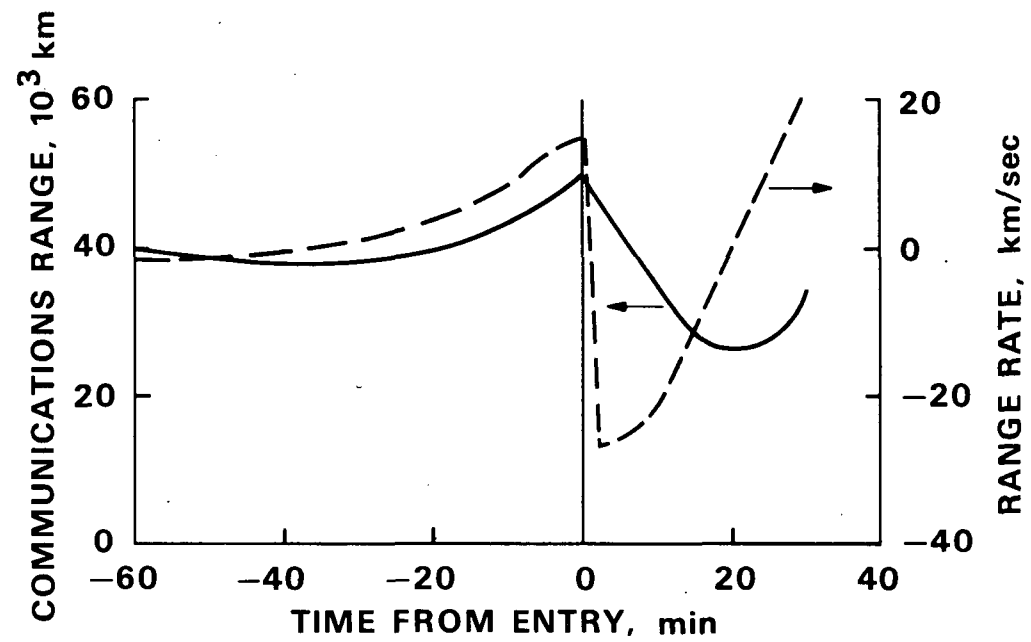


Figure 8. - Communications Range and Range Rate; Nominal Mission.

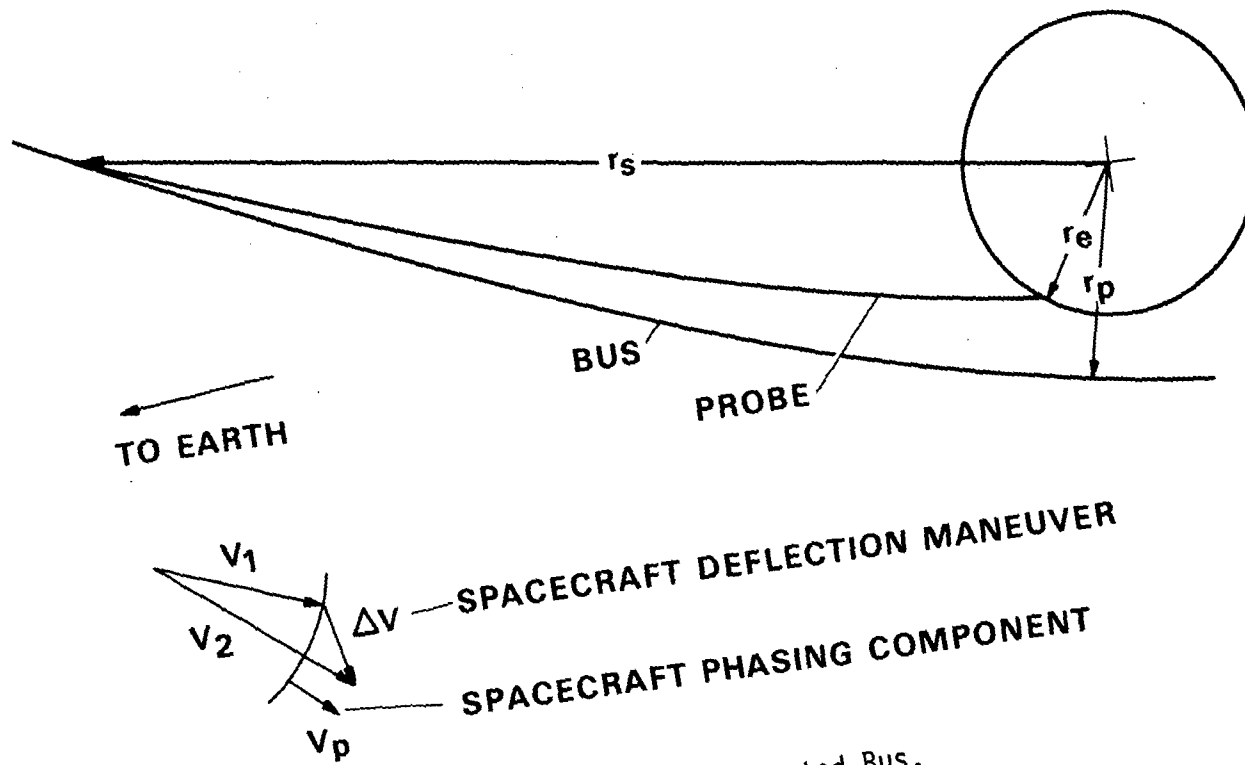


Figure 9. - Deflected Bus.

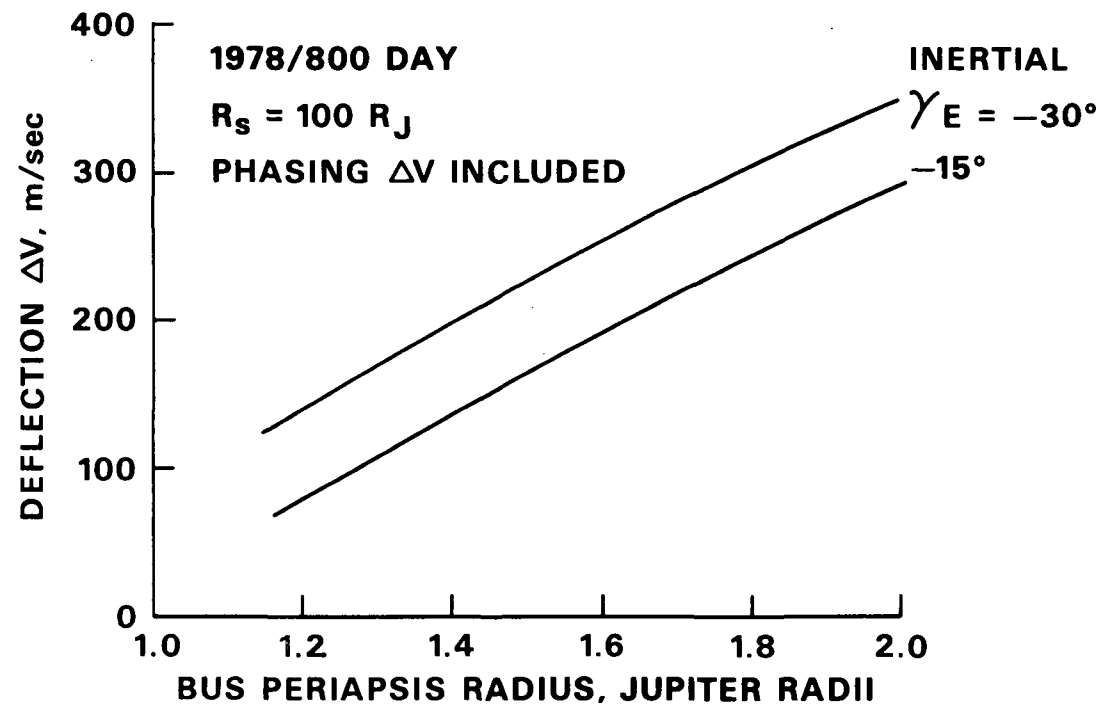


Figure 10. - Deflected Bus ΔV Requirements.

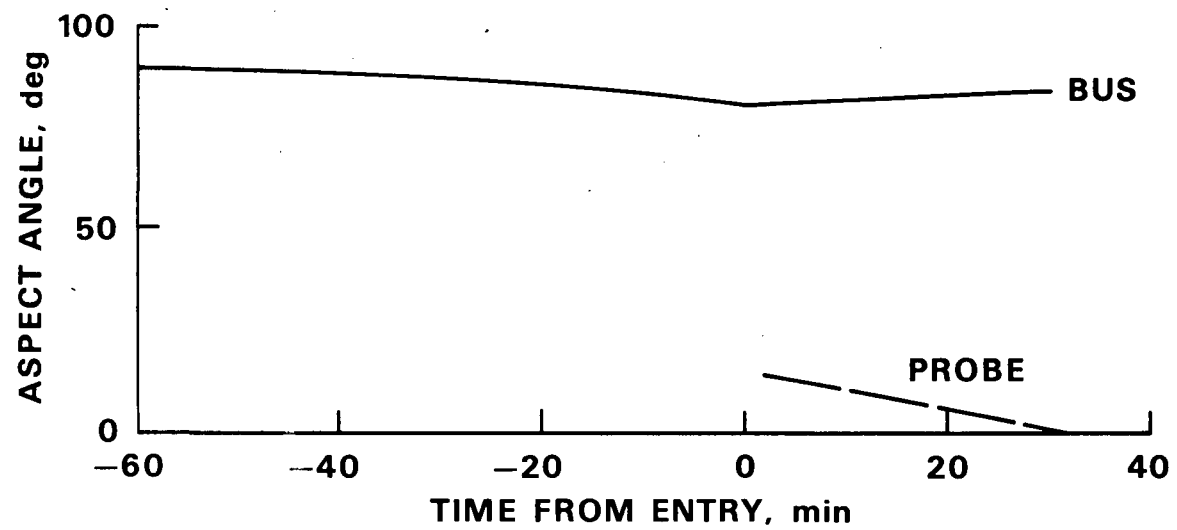


Figure 11. - Communications Geometry; Mission to Limit Radiation Damage.

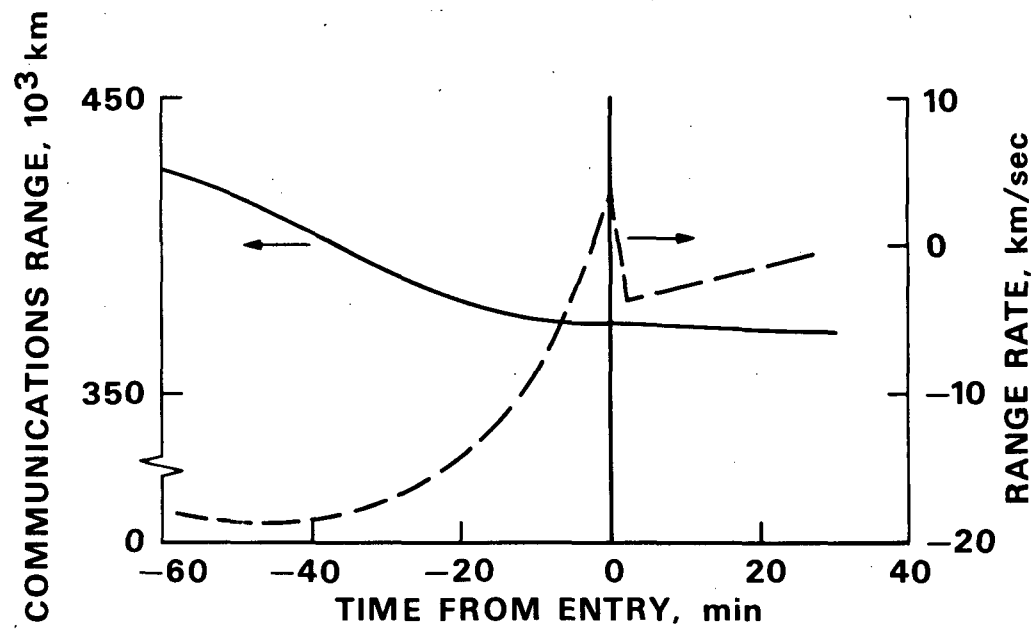


Figure 12. - Communications Range and Range Rate; Mission to Limit Radiation Damage.

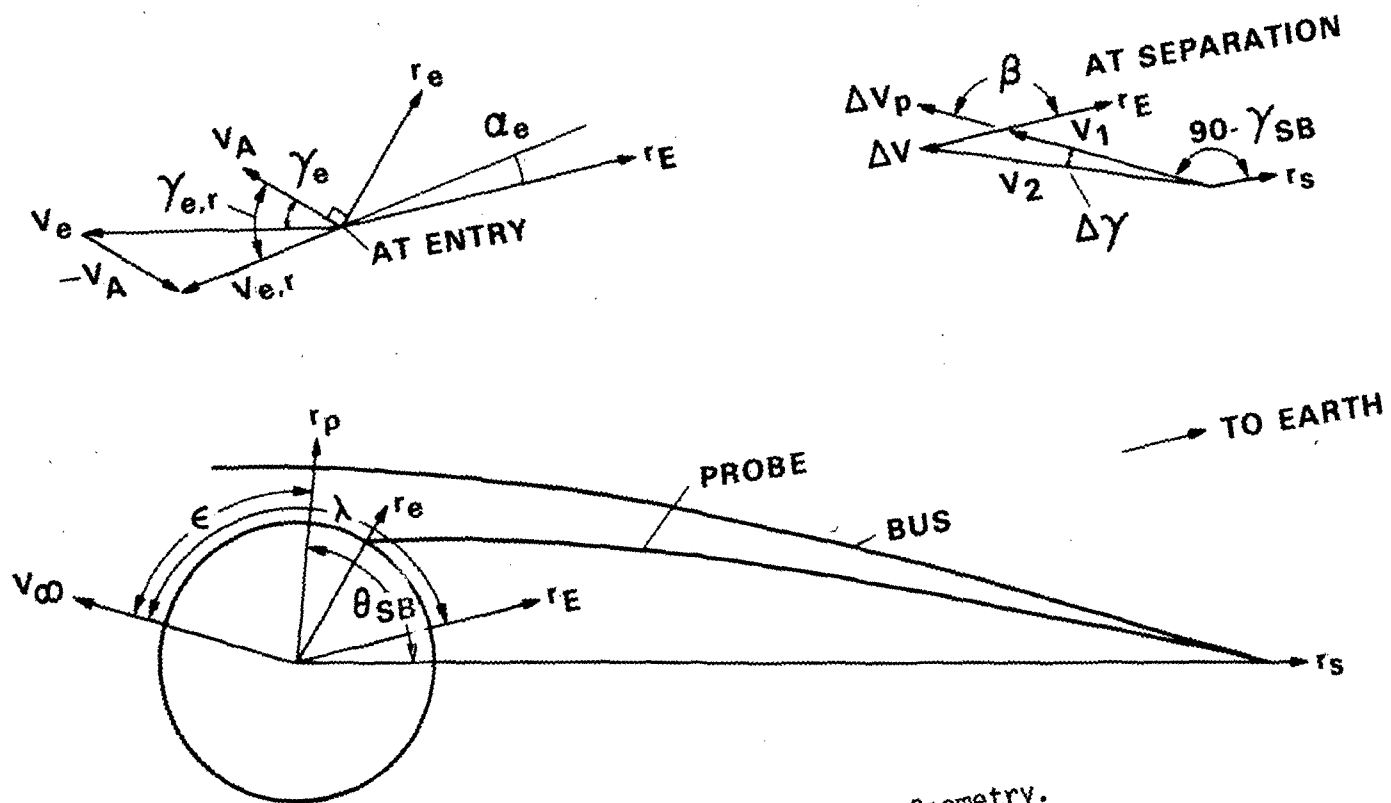


Figure 13. - Deflected Probe Geometry.

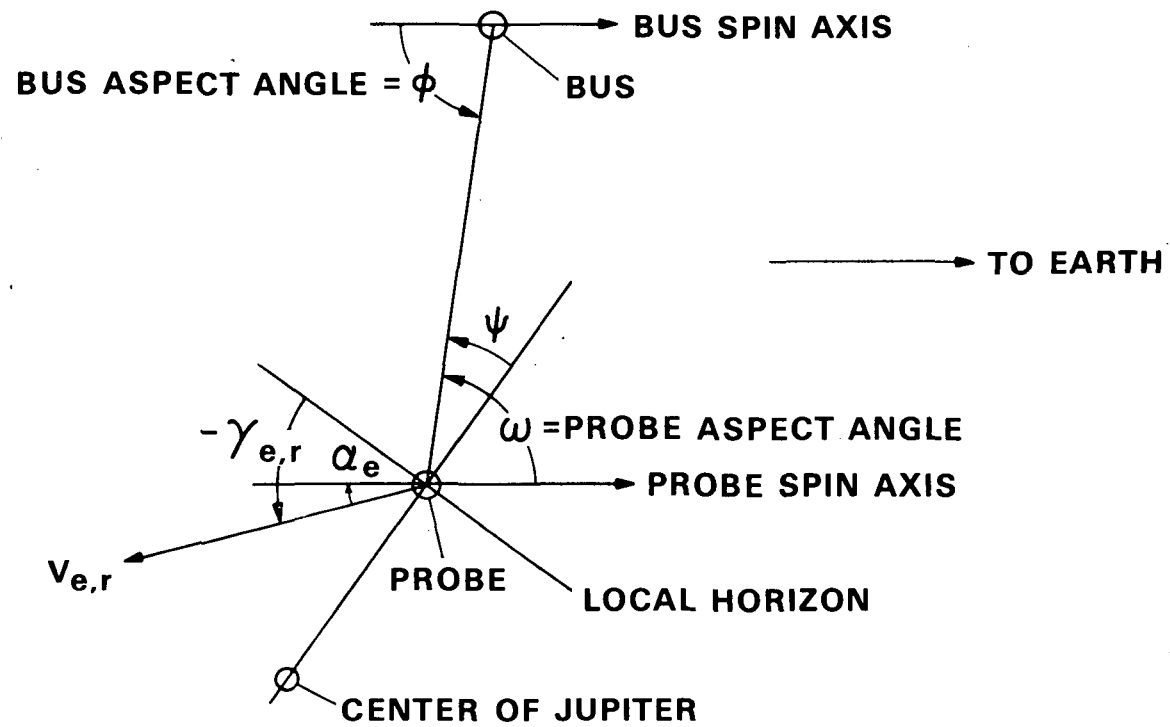


Figure 14. - Aspect Angles; Shown at Time of Entry.